

Dealloying of Platinum-Aluminum Thin Films

Part I. Dynamics of Pattern Formation

Henning Galinski,* Thomas Ryll, Lukas Schlagenhauf, Felix Rechberger, Sun Ying, and Ludwig J. Gauckler
Nonmetallic Inorganic Materials, ETH Zurich, Zurich, Switzerland

Flavio C.F. Mornaghini, Yasmina Ries, and Ralph Spolenak
Laboratory for Nanometallurgy, ETH Zurich, Zurich, Switzerland

Max Döbeli

Ion Beam Physics, ETH Zurich, Zurich, Switzerland

(Dated: May 30, 2018)

Applying focused ion beam (FIB) nanotomography and Rutherford backscattering spectroscopy (RBS) to dealloyed platinum-aluminum thin films an in-depth analysis of the dominating physical mechanisms of porosity formation during the dealloying process is performed. The dynamical porosity formation due to the dissolution of the less noble aluminum in the alloy is treated as result of a reaction-diffusion system. The RBS analysis yields that the porosity formation is mainly caused by a linearly propagating diffusion front, i.e. the liquid/solid interface, with a uniform speed of $v_f = 42(3)$ nm/s when using a 4M aqueous NaOH solution at room temperature. The experimentally observed front evolution is captured by the normal diffusive Fisher-Kolmogorov-Petrovskii-Piskounov (FKPP) equation and can be interpreted as a branching random walk phenomenon. The etching front produces a gradual porosity with an enhanced porosity in the surface-near regions of the thin film due to prolonged exposure of the alloy to the alkaline solution.

PACS numbers: 81.05, 81.07.-b, 81.16.Dn, 61.43Dq, 47.70.Fw, 82.20.Fd, 05.40.-a

Keywords: dealloying, dealloying dynamics, FKPP equation, propagating diffusion front, reaction-diffusion system, rutherford backscattering spectrometry

In his original work, Murray Raney in 1927 dealloyed Nickel-Aluminum alloys with concentrated sodium hydroxide in order to derive extremely porous and nanostructured Nickel catalysts [1]. This process has gained renewed attention in recent years for the formation of porous metallic thin films [2–8]. The interest is not only motivated by industrial needs of miniaturized sensors and catalysts but also by fundamental interests in the physical mechanisms that control the pattern or porosity formation [4, 5]. Dealloying can be interpreted as a reaction-diffusion process, where the less noble metal in a solid solution is dissolved at the solid/liquid interface to an acid or alkaline solution. The reaction and diffusion processes can be treated in one dimension in the case of thin films. For normal diffusion, the reaction-diffusion equation (RDE) reads

$$\frac{\partial}{\partial t}c(x, t) = R(c) + D\Delta_x c(x, t), \quad (1)$$

where $c(x, t)$ is the local concentration, $R(c)$ is a system specific reaction term and D the diffusion coefficient [9–11]. In contrast to its importance to basic mechanisms, reliable measurements of the dealloying dynamics are rare and mostly indirect. It is usually assumed that the dealloying of the less noble metal in the alloy can be treated in terms of a phase separation at the reaction interface via a mean field approach described by the nonlinear Cahn-Hilliard equation [2, 4, 5]. However, there is no experimental data available that conceives the dynam-

ics of dealloying as a direct result of a reaction-diffusion (RD) system. Therefore the main objective of this paper is to prove a relation between the observable macroscopical changes in the composition and morphology of the thin film with the predictions of a reactive-diffusion equation. The Pt/Al system has been selected, since it shows a nearly complete miscibility between the two elements including the formation of various intermetallic phases. Pt/Al layers of 300 nm in thickness, were deposited at room temperature by magnetron co-sputtering ($P_{\text{Pt}} = 37$ W, $P_{\text{Al}} = 252$ W, $p_{\text{Ar}} = 2.6 \cdot 10^{-3}$ mbar) onto amorphous Si_3N_4 substrates that were pre-cleaned using isopropanol and acetone.

In order to achieve a measurement scheme of sufficient significance, the substrates coated with the Pt/Al thin film were dealloyed in 4M NaOH at room temperature in a time domain between 1 – 10 s in steps of $\Delta t = 1$ s. The reaction between the thin film and the basic solution can be established to



The morphological and compositional analysis of the samples was studied via FIB and RBS. Single and multiple cross-sections of the dealloyed Pt/Al systems were cut, polished and imaged using a Zeiss NVISION 40 FIB etching system. The stacks of multiple cross-sections were aligned recursively by Stackreg [12] and reconstructed using AVS Express (Advanced Visual Systems Inc.). The voxel-size of the resulting tomographic images is not cu-

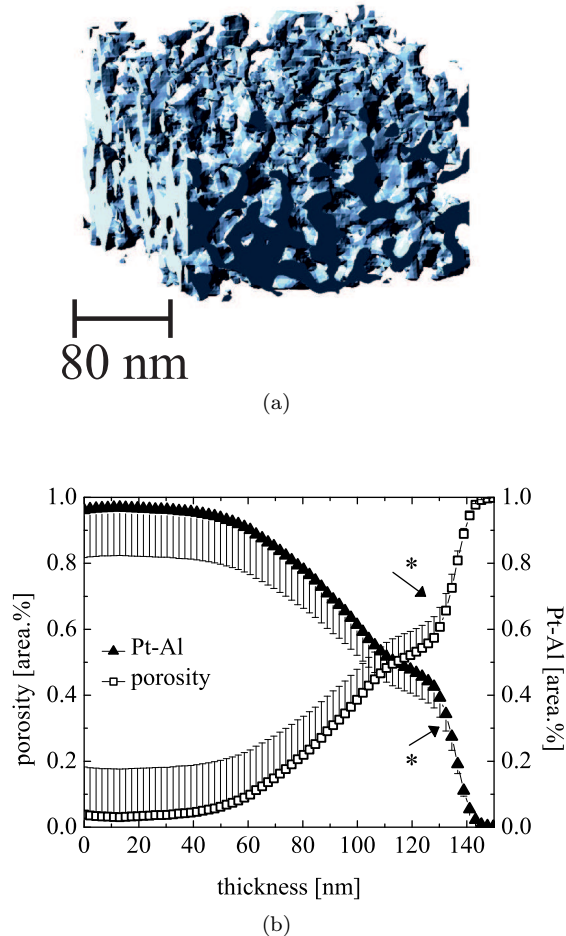


FIG. 1. 1(a) Three-dimensional (3D) reconstruction of a dealloyed 120nm-thick $\text{Pt}_{.72}\text{Al}_{.28}$ film on Si_3N_4 obtained via FIB nanotomography 1(b) Developing of the mean porosity as function of the film thickness. Regions denoted by * indicate deviations due to the dissolution of Pt which caused film shrinkage and a steeper gradient in porosity.

bic and $2.17 \times 2.17 \times 6.5 \text{ nm}^3$ in size. The compositional analysis was performed by RBS experiments using a 2MeV ^4He beam and a standard silicon surface barrier detector at 165° . The background was subtracted using a common fitting procedure [13]. The elemental composition and diffusion profiles were obtained using the RUMP program [14]. For the investigated films RBS provides a quantitative one dimensional depth profile of the composition with a depth resolution of 10 to 20 nm [15].

In Figure 1(a), the spatial arrangement of the PtAl-phase as obtained by the FIB-nanotomography reconstruction after 10 s of dealloying is shown. The dealloying results in a fine branch-like pattern with a median branch thickness of 15 – 20 nm. The formed pattern is non-uniform and characterized by a strong directive gradient porosity as function of the film thickness h . This gradient porosity,

as shown in Figure 1(b), is substantiated by calculating the porosity from multiple cross-sections of the dealloyed Pt/Al film. The porosity is increasing with increasing film thickness h and in the vicinity of the film/ambient interface a zone of $\approx 25 \text{ nm}$ thickness is observed where the porosity evolution changes its functional shape significantly. The zone denoted by * in Figure 1(b) is assumed to originate due to the prolonged exposure to the alkaline solution that caused the nearly complete dissolution of the Al in the film which consequently led to the dissolution of the Pt and thus to a shrinkage of the film.

In order to further evaluate the dynamics of pattern formation, time-resolved RBS spectra have been measured and analyzed using the RUMP software. From the simulated spectra, critical time-dependent measurands like the spatial composition η , the thickness of each layer h , the diffusion coefficient D and additional loss of Al in

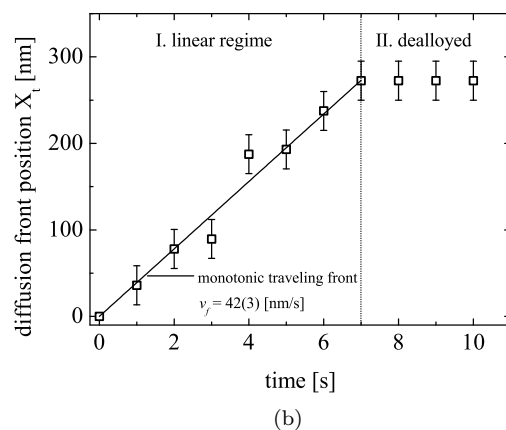
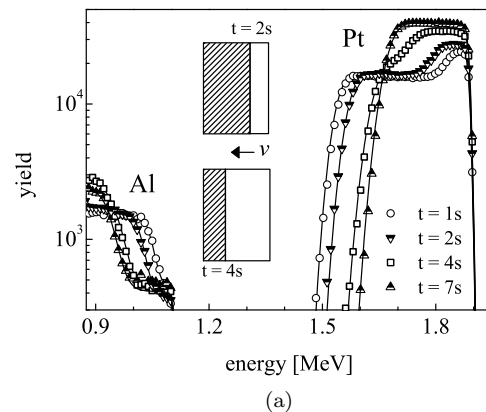


FIG. 2. 2(a) Plot of the subtracted 2MeV ^4He RBS spectra of the time-resolved dealloying of Pt/Al thin films (dots) and simulated spectra (solid lines) using RUMP. 2(b) Propagation front velocity $v_f = \partial_t X_t$ derived from the shrinkage-corrected front positions X_t obtained by RUMP simulations

TABLE I. Measured initial and final alloy compositions $\eta_{0,\text{end}}$, diffusion front velocity v_f , film shrinkage and the diffusion coefficient D .

η_0 [at.%]	η_{end} [at.%]	v_f [nm/s]	$\partial_t h$ [nm/s]	D [m^2/s]
Pt _{0.24} Al _{1.76}	Pt _{0.72} Al _{1.28}	42(3)	-25(3)	$4.2(13) \cdot 10^{-17}$

the dealloyed layer have been determined. The position of the dissolution front X_t is calculated with respect to the initial film thickness h_0 and thus considers a possible layer shrinkage in the dealloyed layer. The resulting RBS spectra and their corresponding simulation using η , h , X_t as fitting parameters are shown in Figure 2(a).

The RBS spectra verify not only the dissolution of Al as function of time but also a step-like profile in the Pt-peak which can be attributed to the position X_t of the traveling diffusion front during dealloying. In addition a shrinkage of the Pt/Al film in the order of $-25(3)$ nm/s is indicated, which is a direct result of the measured additional Al-loss of 0.02 at.%/s in the already dealloyed layer. These results are in accordance to the microstructural findings in Figure 1 and present clear evidence that the formed pattern is not solely defined by the reactive processes close to the propagation diffusion front but also by diffusion processes in the bulk of the alkaline solution. As shown in Figure 2(b), the shrinkage-corrected position X_t of the travelling diffusion front scales linearly with time t and the corresponding velocity of this monotonic travelling front is $v_f = \partial_t X_m = 42(3)$ nm/s. All relevant data have been summarized in Table I.

The experimental observation of an initially flat liquid/film interface that evolves with time to a propagating diffusion front with a constant front velocity v_f are specific characteristics of the Fisher-Kolmogorov-Petrovskii-Piskounov (FKPP) equation obeying a traveling wave solution with $u(x, t) = \psi(x - v_f t)$ [16]. The FKPP equation reads as follows

$$\frac{\partial}{\partial t} u(x, t) = D \Delta_x u(x, t) + \mu u(x, t)(1 - u(x, t)), \quad (3)$$

where D is a diffusion coefficient and μ represents the reaction rate of the system. The FKPP equation is a well known and widely applied nonlinear reaction-diffusion equation [9, 17]. Using structural stability arguments [18], it can be shown that the front velocity v_f is solely defined by the reaction rate μ and the diffusion coefficient D and reads

$$v_f = 2\sqrt{\mu D}. \quad (4)$$

Using the experimental values for v_f and D , the reaction rate of the dealloying system is determined to $\mu = 11.0(8)$ at.%/s. Thereafter Equation 3 has been solved numerically using Mathematica with a Heaviside step function $H(x)$ as initial condition $u(0, t) = 1 - H(x)$. To match the experimental conditions though, the corresponding solutions is established to be $c(x, t) = 1 -$

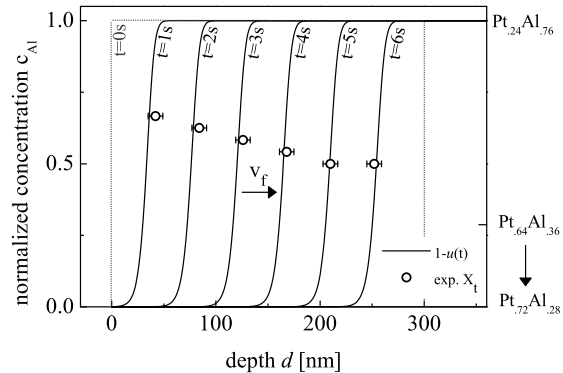


FIG. 3. Comparison of the diffusion fronts obtained by numerical solution of 3 in the case of $\mu = 11.0(8)$ at.%/s and $D = 4.2(13) \cdot 10^{-17}$ m^2/s with front positions X_t calculated using v_f .

$u(x, t)$. In Figure 3 $c(x, t)$ with $\mu = 11.0(8)$ at.%/s and $D = 4.2(13) \cdot 10^{-17}$ m^2/s have been plotted in comparison to the experimentally determined front positions X_t . The chosen reactive diffusion equation fits nicely to the measured diffusion front positions X_t , although it does not feature the measured additional Al-loss in the early stage of dealloying. By choosing $c(x, t) = 1 - u(x, t)$ the reaction term of the RD system becomes $R(C) = \mu c(x, t)(c(x, t) - 1)$, this kind of reaction-diffusion systems describe branching random walks [19]. In the present case the branching event is assumed to be the dissolution of Al out of the Pt/Al alloy whose space is then occupied by the alkaline solution. Thereby the spatial occupation grows linearly with time [20], as also proven experimentally in Figure 3.

In essence, it has been shown that consistent with the experimental findings, the dynamics of dealloying can be treated as a reaction-diffusion system. Thereby the used FKPP equation reproduces the experimental characteristics in a satisfactory manner. The RD-system is fully defined by the measured propagation front velocity $v_f = 42(3)$ nm/s and the diffusion coefficient $D = 4.2(13) \cdot 10^{-17}$ m^2/s .

In addition, experimental evidence has been found that the pattern formation related to the dealloying process can be regarded as a superposition of the reaction-diffusion system confined to the solid/liquid interface and an additional slower dissolution process with 0.02 at.%/s in the bulk of the alkaline solution. This process is much slower than the propagating diffusion front but it has a severe impact on the end-form of the dealloyed pattern and the porosity distribution.

In an upcoming work, the obtained dealloyed films are analyzed in matters of their catalytical properties and stability during an oxygen reduction reaction (ORR). The authors greatly acknowledge the financial sup-

ported by the Swiss Bundesamt für Energie (BfE), Swiss Electric Research (SER), the Competence Center of Energy and Mobility (CCEM) and the Swiss National Foundation (SNF). We would like to thank the EMEZ (Electron Microscopy Center, ETH Zurich) for their support. Henning Galinski would like to thank Anna Evans, Iwan Schenker and Barbara Scherrer for fruitful and stimulating discussions.



* henning.galinski@mat.ethz.ch

- [1] M. Raney, US Patent **1628190** (1927).
- [2] J. Erlebacher, M. J. Aziz, A. Karma, N. Dimitrov, and K. Sieradzki, *Nature* **410**, 450 (2001).
- [3] J. Erlebacher, in *Nanoscience and Nanotechnology* (CRC Press, 2008) pp. 2938–2946–.
- [4] J. Erlebacher, *J. Electrochem. Soc.* **151**, C614 (2004).
- [5] C. Eilks and C. Elliott, *J. Comput. Phys.* **227**, 9727 (2008).
- [6] A. J. Forty, *Nature* **282**, 597 (1979).
- [7] M. C. Simmonds, H. Kheyrandish, J. S. Colligon, M. L. Hitchman, N. Cade, and J. Iredale, *Corros. Sci.* **40**, 43 (1998).
- [8] J. C. Thorp, K. Sieradzki, L. Tang, P. A. Crozier, A. Misra, M. Nastasi, D. Mitlin, and S. T. Picraux, *Appl. Phys. Lett.* **88**, 033110 (2006).
- [9] R. D. Benguria and M. C. Depassier, *Phys. Rev. Lett.* **77**, 1171 (1996).
- [10] R. Fisher, *Annals of Eugenics* **355** (1937).
- [11] C. R. Doering, C. Mueller, and P. Smereka, *Physica A* **325**, 243 (2003).
- [12] P. Thévenaz, U. Ruttimann, and M. Unser, *IEEE T. Image. Process.* **7**, 27 (1998).
- [13] M. Döbeli, *Nucl. Instrum. Methods Phys. Res., Sect. B* **249**, 800 (2006).
- [14] L. R. Doolittle, *Nucl. Instrum. Methods Phys. Res., Sect. B* **15**, 227 (1986).
- [15] M. A. N. Yongqiang Wang, *Handbook of modern ion beam materials analysis* (Materials Research, Warrendale, Pa., 2009).
- [16] W. van Saarloos, *Phys. Rev. A* **39**, 6367 (1989).
- [17] A. Lemarchand, A. Lesne, and M. Mareschal, *Phys. Rev. E* **51**, 4457 (1995).
- [18] G. C. Paquette, L.-Y. Chen, N. Goldenfeld, and Y. Oono, *Phys. Rev. Lett.* **72**, 76 (1994).
- [19] E. Brunet and B. Derrida, *Europhys. Lett.* **87**, 60010 (2009).
- [20] H. P. McKean, *Commun. Pure Appl. Math.* **28**, 323 (1975).